

# Image-Based Analysis of Condensation on In-Vessel Passive Containment Cooling Systems in the PANDA Facility

Isabella Feagan\*, Yago Rivera, Nabil Ghendour and Ralf Kapulla

PSI Center for Nuclear Engineering and Sciences, 5232 Villigen PSI, Switzerland

## Abstract

Passive Containment Cooling Systems (PCCS) enhance the safety of advanced nuclear reactors by removing heat through the condensation of steam. To support the development and validation of such systems, this research presents an experimental study performed at the large-scale PANDA facility, focused on capturing detailed observations of condensation phenomena on an in-vessel PCC pipe. A key feature of this campaign is the application of a high-resolution optical imaging system capable of capturing local liquid film dynamics in a large-scale setup – an approach rarely studied at this scale. The experiment simulates a steam release into containment, with a single, highly instrumented PCC pipe maintained at constant inlet temperature to provide well-defined boundary conditions. Image sequences were acquired at several pressure levels during a controlled transient, and analyzed to extract interfacial wave celerity, frequency content, and film thickness. The results reveal the formation and propagation of surface waves along the condensate film, with dominant wave frequencies around 5 Hz and average celerities near 1 m/s. These measurements provide a valuable dataset for improving interfacial modeling in condensation processes and offer a basis for validating CFD and system-level simulation tools applied to passive containment cooling analysis.

**Keywords:** Passive Containment Cooling System; Optical techniques; Containment; Thermal-hydraulics; CFD validation; PANDA facility

## 1 Introduction

Passive safety systems are an important feature of modern nuclear reactor designs, intended to maintain core and containment integrity during accident scenarios without reliance on active components. Among these, Passive Containment Cooling Systems (PCCS) facilitate heat removal from the containment through steam condensation and natural circulation, helping to mitigate pressure buildup and preserve containment integrity over extended periods, [1, 2].

PCCS are not widely implemented in the current fleet of operating Light Water Reactors (LWRs), which predominantly rely on active cooling methods. While some Generation III+ designs include PCCS, their adoption remains limited. In contrast, many Small Modular Reactor (SMR) concepts incorporate passive safety systems as a core feature, though most are at present in the development or licensing stage. Advancing these technologies requires high-quality experimental data and validated models to demonstrate performance and support regulatory approval under varied accident conditions.

The performance of PCCS is governed by complex thermo-hydraulic phenomena, including condensation, liquid film formation, interfacial waves, and flow instabilities within natural circulation loops. These processes are influenced by system configuration, pressure conditions, and the characteristics of the heat sink. Variations in operating conditions can induce flow oscillations, stratification, or reduced heat transfer efficiency, all of which may compromise system reliability, [3]. Computational tools such as system codes and Computational Fluid Dynamics (CFD) simulations are used to analyze these behaviors, but their predictive capabilities depend on experimental validation. Programs like the OECD/NEA PANDA Project address this need by providing benchmark data. Within this framework, one of the experimental series at the PANDA facility investigates the behavior of a simplified

\*Speaker. Email: [isabella.feagan@psi.ch](mailto:isabella.feagan@psi.ch)

in-vessel PCC system under quasi-steady and transient conditions to improve the understanding of natural circulation and condensation processes relevant to containment cooling.

Most studies on PCCS have focused on global parameters such as pressure, temperature, and overall heat transfer, [4, 5]. However, detailed knowledge of local condensation behavior, including the liquid film characteristics and interfacial dynamics, is critical for refining heat transfer models. Properties such as wave structures, frequency content, and film thickness directly affect condensation performance but are difficult to measure with conventional sensors, [6], to support the improvement of condensation models and contribute to the validation of simulation tools for passive containment cooling systems. To capture these phenomena, we applied an optical imaging system at the PANDA facility, enabling visualization of the liquid film along the PCC pipe.

## 2 Experimental setup

The experimental setup for the the test was implemented in the large-scale PANDA facility. The specific objective of the test was to simulate the release of steam into the containment in the event of an accident, in the presence of an in-vessel passive condenser. The experimental data are intended to support the validation and coupling of system codes with CFD models, providing detailed information on the condensation process at the pipe scale. To facilitate this, the condenser system was designed around a single, highly instrumented PCC pipe, with conditions set to maintain a constant inlet temperature. The experimental conditions were designed to avoid boiling inside the pipe, thereby simplifying the boundary conditions for CFD analyses.

The experimental configuration consisted of a large vessel approximately 4 m in diameter and 8 m in height, supplied with steam. Steam was injected into the vessel at a point located one meter from the wall and positioned opposite to the passive condenser. The PCC pipe, designed specifically for these experiments, has an internal diameter of 37.2 mm and features a 6-meter vertical section exposed within the vessel for steam condensation. The remainder of the pipe was fully insulated along its length. The cooling system was connected to two interconnected water pools located above the vessel, ensuring a stable and controlled inlet temperature for the condenser. The experimental setup outline is provided in Figure 1 a).

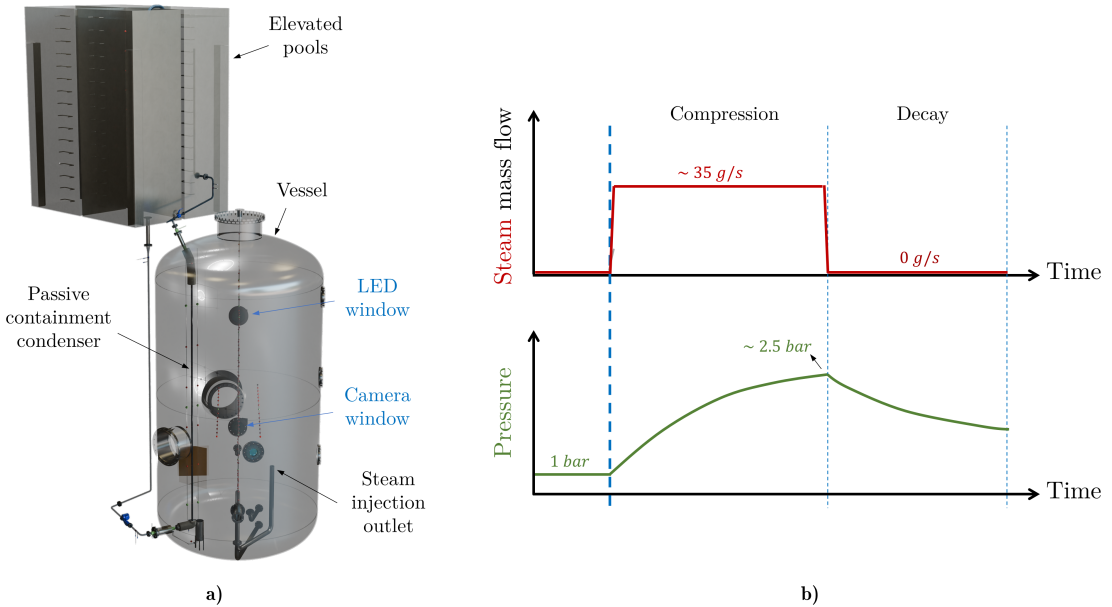


Figure 1: Outline illustrating the various components that are involved in the test configuration, a); Generic test procedure of the experiment, b).

The test procedure began with a preconditioning phase, heating the vessel to approximately  $135\text{ }^{\circ}\text{C}$  to avoid condensation on the vessel walls and establishing an internal atmosphere of 100% steam at  $1\text{ bar}$ . Once these conditions were reached, the main transient phase started with steam injected at  $35\text{ g/s}$ . This injection rate was set to exceed the heat removal capacity of the PCC pipe, resulting in a pressure increase inside the vessel. Steam injection continued until the system reached  $2.5\text{ bar}$ , after which the injection was halted. The system was then left to passively decay, with the PCC pipe continuing to remove heat and allowing the vessel pressure and temperature to decrease over time, Figure 1 b).

### 3 Methodology

The experimental campaign included a broad set of measurements – over one hundred temperature sensors, gas concentration, pressure, mass flow rates, and condensate collection – complemented by a high-resolution optical imaging system designed to observe the liquid film on the PCC pipe (Figure 2). The setup featured a Basler ace 2 a2A1920-160umPRO camera ( $1200 \times 1936\text{ px}$ ), mounted externally with a direct view of the condensation region through a dedicated optical port. A  $150\text{ mm}$  focal length lens provided a detailed  $200\text{ mm}$  field of view over the region of interest. Illumination was supplied by an IL-105/6X LED in continuous mode, positioned coaxially with the camera to backlight the vessel.

During the experiment, an image series was taken at each interval of  $0.25\text{ bar}$  to capture the changing behavior of the liquid film. Each recording of 1024 frames was taken at a frame rate of  $96\text{ fps}$ , resulting in recordings with a duration of  $10.67\text{ s}$ . At this frame rate, the camera was able to capture images resolving the dynamic behavior of the liquid film and the falling surface waves. The careful optimization and design of the optical system enabled close-up measurements that are rarely feasible in large-scale facilities such as PANDA. As a result, it became possible to extract quantitative information on the condensate liquid film from the acquired images.

DaVis 8.4 was first used to extract a slice of 40 to 55 pixels from the image, isolating the left side of the pipe where image contrast was the highest between the lighter background and darker liquid film. Additionally, a simple calibration was performed to convert pixels to millimeters using the pipe's outer diameter of  $42.4\text{ mm}$  as a reference.

Using the sliced image, a simple edge detection method implemented in MATLAB was used to extract the liquid film boundary from the image. This process is shown in Figure 3, where the final plot in the series is the extracted edge data smoothed using a three pixel moving average. The minimum liquid film boundary detected throughout the entire series was used to roughly estimate the thinnest liquid film detected or the solid pipe wall, and to obtain a zero point for the liquid film thickness.

MATLAB was used for post-processing and analysis. Firstly, a peak detection algorithm identified wave peaks as local maxima, enabling tracking along the pipe length. Peaks persisting for at least five frames were classified as surface waves and used to compute celerity from their displacement and the known sampling rate ( $96\text{ Hz}$ ), as shown in Figure 4. This process was repeated to obtain average celerity values for each pressure level. Since these interfacial waves stem from flow instabilities, their celerity differs from the bulk film velocity.

To estimate dominant wave frequencies, Welch's method was applied to the temporal film thickness signal using 256 samples with 50% overlap with a Hamming window. Power spectral density (PSD) plots were computed per vertical row and then averaged across the pipe height to yield a representative spectrum for each pressure level.

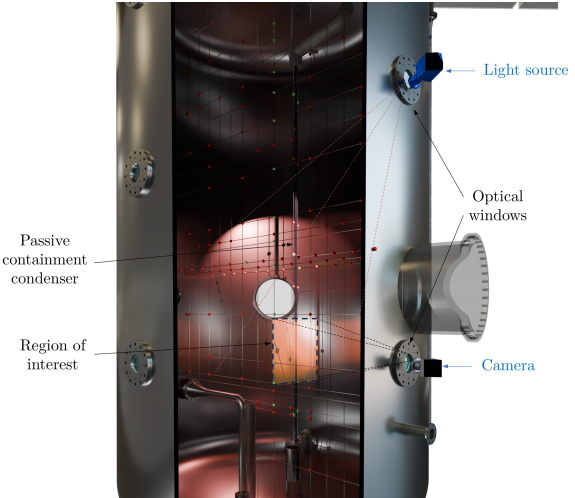


Figure 2: Arrangement of the imaging system setup for the experiments.

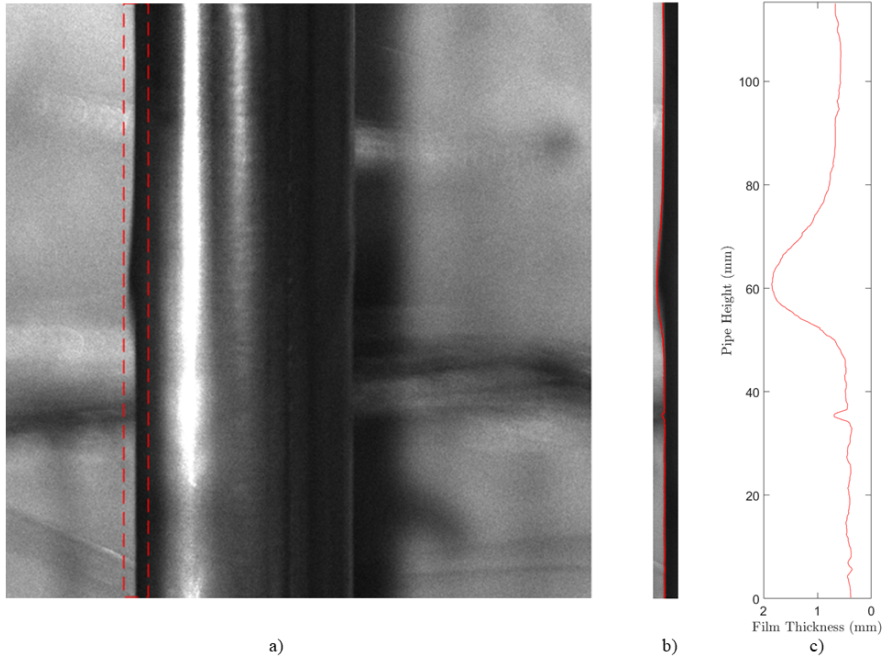


Figure 3: Demonstration of film edge detection algorithm; a) Raw image with extracted slice shown in the red region; b) Extracted slice with edge detected, shown in red; c) Magnitude of the liquid film, where  $x = 0$  represents a rough estimate of the pipe surface below the liquid film.

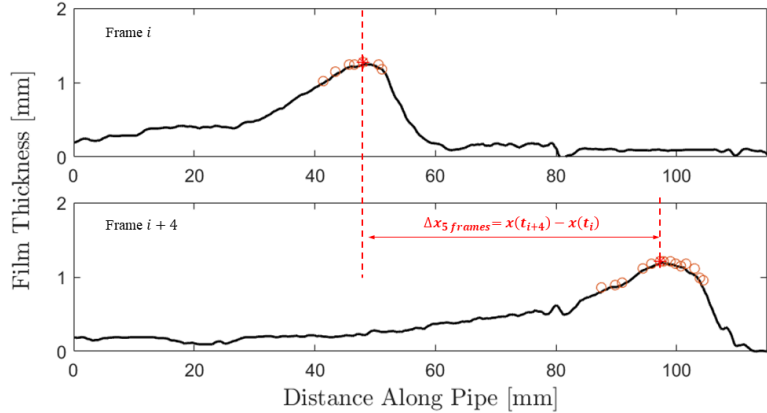


Figure 4: Peak detection algorithm for wave celerity calculation. Distance traveled by a wave is found using the maximum peak determined from the first and last frame in a five-frame series.

## 4 Results and discussion

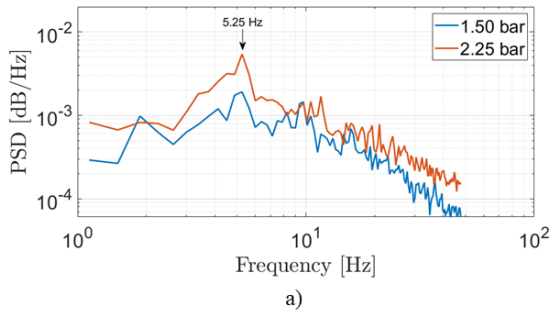
The analysis is limited to the recordings taken from 1.50 bar to 2.50 bar, where a stable liquid film was consistently present along the PCC pipe.

A space-time plot of the film thickness signal for one representative case is presented in Figure 5. The film thickness is color-coded with time on the x-axis and vertical pipe position on the y-axis. The inclined streaks in the plot represent the propagation of surface waves, with their slope relating to the wave celerity. The regularity of spacing suggests a relatively consistent wave period, and the absence of merging or splitting waves supports the identification of a dual-wave regime. This regime is characterized by large-amplitude waves separated by relatively quiescent film regions, as reported in [7]. The underlying temporal film thickness signal further confirms this behavior, highlighting the

temporal passage of surface waves and smaller-scale ripples. Based on rough estimates of the film Reynolds number ( $Re_{film} \approx 450\text{--}730$ ), the flow regime aligns well with the dual-wave regime.

The frequency content of the surface waves was examined using Welch's method to compute the PSD, as shown in Figure 6 a). Across all pressures, a dominant frequency band is observed between  $3\text{--}6\text{ Hz}$ , with a consistent peak around  $5\text{ Hz}$ . Although wave generation in such flows is not strictly periodic, the PSD suggests bounded variability in wave frequencies. The stable spectral features identified indicate that wave dynamics are largely governed by film instabilities rather than external influences such as shear from gas flow.

The average wave celerities, extracted from peak tracking (Figure 4), are presented in Figure 6 b). Across the tested pressure range, values remain close to  $1\text{ m/s}$ , with a slight increasing trend at higher pressures. This behavior is consistent with expectations for laminar falling films, where film thickness increases with condensation rate scaling approximately as  $m^{1/3}$  [8]. As a result, even a significant change in condensate flow, estimated for this experiment around  $\approx 65\%$  from  $1.5$  to  $2.5\text{ bar}$ , corresponds to a relatively moderate increase in film thickness ( $\approx 15\%$ ). A thicker film tends to reduce wall friction effects, contributing to a mild increase in wave celerity. Additionally, in the present configuration, there is no significant shear imposed by gas flow along the interface, which would otherwise strongly influence wave behavior. Such a modest change is unlikely to induce significant variation in wave celerity. Although increasing the film thickness can slightly reduce wall friction, the overall effect on wave speed, as shown in Figure 6 b) is modest.



a)

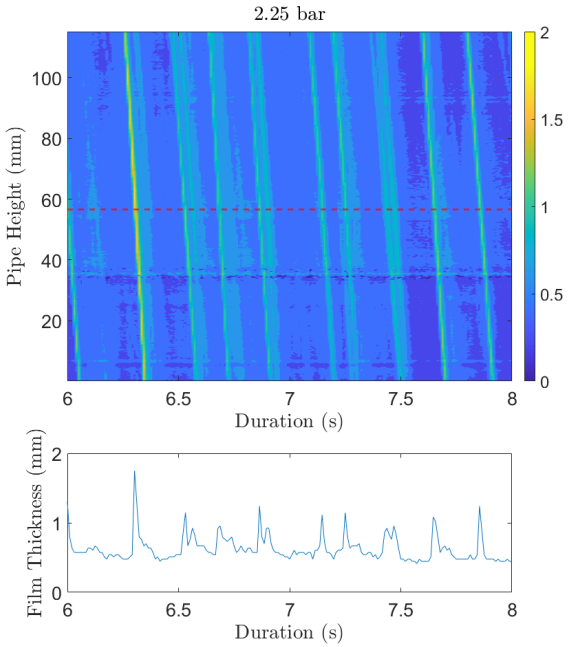


Figure 5: Spacetime plot of interfacial wave thickness obtained from the series taken at  $2.25\text{ bar}$  over a duration from  $4\text{ s}$  to  $6\text{ s}$ . Time is shown along the x-axis and axial position along the pipe height in the y-axis. The color map indicates the local film thickness, given in mm, showcasing the propagation of the liquid film surface waves over time. Below this plot, the corresponding film thickness signal halfway through the ROI.

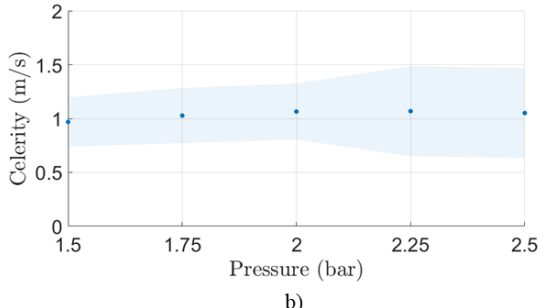


Figure 6: PSD comparing dominant liquid film wave frequencies at  $1.50\text{ bar}$  and  $2.25\text{ bar}$  a), and celerity trend observed b).

## 5 Conclusions

The experimental campaign at the large-scale PANDA facility has demonstrated that high-resolution optical diagnostics can effectively capture detailed condensation phenomena on the surface of a PCCS condenser – such as interfacial wave celerity and frequency – even within a complex, large-scale environment. By resolving sub-millimeter liquid films on a  $42.4\text{ mm}$  diameter PCC pipe inside a  $4\text{ m} \times 8\text{ m}$  vessel, the study provides quantitative evidence of surface wave behavior, with wave celerities around  $1\text{ m/s}$  and dominant frequencies near  $5\text{ Hz}$ , consistent with theoretical expectations for laminar falling films.

These results highlight the potential of a well-optimized imaging setup to yield valuable local-scale data in environments typically dominated by global measurements. When integrated with the broader dataset of system-level parameters such as temperature, pressure, composition, and condensate flow, this information contributes meaningfully to the experimental basis needed to support the validation of CFD and system codes. As such, the campaign represents an important step toward improving the predictive capabilities of models used in the assessment of in-vessel PCCS performance and supports ongoing development of passive safety technologies in nuclear reactor design.

## References

- [1] IAEA, Passive safety systems and natural circulation in water cooled nuclear power plants, International Atomic Energy Agency, OCLC: 526091355.  
URL <https://www.iaea.org/publications/8192>
- [2] IAEA, Passive safety systems in water cooled reactors: An overview and demonstration with basic principle simulators.  
URL <https://www.iaea.org/publications/13530>
- [3] S. Bhattacharyya, D. N. Basu, P. K. Das, Two-phase natural circulation loops: A review of the recent advances 33 (4) 461–482, publisher: Taylor & Francis \_eprint: <https://doi.org/10.1080/01457632.2012.614155>. doi:10.1080/01457632.2012.614155.  
URL <https://doi.org/10.1080/01457632.2012.614155>
- [4] V. Kouhia, V. Riikonen, O.-P. Kauppinen, J. Telkkä, J. Hyvärinen, PASI – a test facility for research on passive heat removal 383 111417. doi:10.1016/j.nucengdes.2021.111417.  
URL <https://www.sciencedirect.com/science/article/pii/S0029549321003691>
- [5] M. Haag, P. K. Selvam, S. Leyer, Effect of condenser tube inclination on the flow dynamics and instabilities in a passive containment cooling system (PCCS) for nuclear safety 367 110780. doi:10.1016/j.nucengdes.2020.110780.  
URL <https://www.sciencedirect.com/science/article/pii/S0029549320302740>
- [6] Y. Rivera, M. Bidon, J.-L. Muñoz-Cobo, C. Berna, A. Escrivá, A comparative analysis of conductance probes and high-speed camera measurements for interfacial behavior in annular air–water flow 23 (20) 8617, number: 20 Publisher: Multidisciplinary Digital Publishing Institute. doi:10.3390/s23208617.  
URL <https://www.mdpi.com/1424-8220/23/20/8617>
- [7] I. Zadrazil, C. N. Markides, An experimental characterization of liquid films in downwards co-current gas–liquid annular flow by particle image and tracking velocimetry 67 42–53. doi:10.1016/j.ijmultiphaseflow.2014.08.007.  
URL <https://www.sciencedirect.com/science/article/pii/S0301932214001499>
- [8] W. Nusselt, Die Oberflächenkondensation des Wasserdampfes, VDI, google-Books-ID: m8fwjgEACAAJ.